Journal of Vibration Engineering & Technologies (2021) 9:73–84
https://doi.org/10.1007/s42417-020-00211-8

ORIGINAL PAPER

Study on Torsional Vibration of RV Reducer Based on Time-Varying Stiffness

Song Wang[1] · Jing Tan[1] · Jingjun Gu[1] · Dishan Huang[1]

Received: 19 March 2020 / Revised: 25 April 2020 / Accepted: 2 May 2020 / Published online: 4 June 2020

Abstract

Purpose The torsional vibration of RV reducer is the key factor affecting the positioning accuracy and trajectory accuracy of industrial robots. It is of great significance to study the torsional stiffness periodic fluctuation and parametric torsional vibration to improve the torsional vibration performance and transmission accuracy of RV reducer.

Methods Based on the torsional stiffness test device of RV reducer, the torsional stiffness is measured and the torsional stiffness curve with periodic fluctuation is obtained. The trigonometric function fitting and mathematical description of torsional stiffness curve are carried out, and the torsional vibration equation of RV reducer parameters is established. The parametric torsional vibration response of RV reducer is simulated by Runge–Kutta method, and the combined frequency characteristics and system stability are analyzed. The torsional vibration test device of RV reducer is developed to study the torsional stiffness fluctuation and torsional vibration fault.

Results The torsional stiffness fluctuation of RV reducer can be divided into a short period and long period, corresponding to different manufacturing errors, and the mechanism of torsional stiffness fluctuation is found out. The frequency spectrum of torsional vibration under working condition is highly consistent with the simulated response spectrum, and the harmonic resonance interval obtained by frequency sweeping is close to the peak of the torsional vibration–speed curve, so the correctness of the established torsional vibration model is verified. Using the mechanism of RV reducer stiffness fluctuation to realize rapid diagnosis of defective parts of RV reducer has a strong engineering application value.

Conclusion The time-varying torsional stiffness of RV reducer will cause the phenomenon of parametric torsional vibration. The vibration response characteristic frequency is a linear combination of internal reference variation frequency and external excitation frequency. The parametric torsional vibration will cause the harmonic resonance of RV reducer and aggravate the torsional vibration. Therefore, it is of great engineering value to study the time-varying torsional stiffness and torsional vibration of RV reducer.

Keywords RV reducer · Time-varying torsional stiffness · Parametric torsional vibration · Vibration spectrum · Property of torsional vibration–speed

Introduction

Industrial robots have been widely used in many fields such as the national defense industry, equipment manufacturing industry, aerospace industry, electronics and electrical industry [1]. As the application of industrial robots more precision, more strict requirements are put forward on the robot's stability. Therefore, the present research task focus on improving the robot dynamic characteristic of the core driving part namely the RV reducer, to ensure the reliability of products, quality stability, and reduce the impact and torsional vibration in the operation and improve the end of the robot running track and position precision [2, 3].

RV reducer is developed on the basis of cycloid-pin planetary reducer. It is a closed two-stage transmission device composed of planetary gear drive and cycloidal-pin drive. RV reducer has a complex and compact structure and high matching accuracy. Compared with the general planetary transmission, it has many advantages such as large deceleration ratio, high transmission efficiency, gentle movement, small return difference and large bearing capacity [4].

✉ Dishan Huang
hdishan@shu.edu.cn

[1] Mechanical Engineering and Automation, Shanghai University, Shanghai 200444, China

Torsional stiffness is an important performance of RV reducer [5, 6]. Excessive fluctuation of torsional stiffness leads to parametric torsional vibration of RV reducer, and it induces the flutter of the industrial robot system and affects the positioning accuracy and trajectory accuracy seriously.

Based on Hertz formula and Ishikawa formula, Zhang [7] established a 5-DOF torsional dynamic model of RV-6AII reducer under load. The concept that torsional stiffness changes periodically with time was put forward earlier, which provided a new idea for torsional stiffness modeling of RV reducer, but no explicit torsional stiffness model was established. Park [8] established the semi-analytical torsional stiffness model according to the topology characteristics of RV reducer. On the basis of Park's model, Kim [9] considered the bearing elasticity at the hinge of cycloid gears and crank shafts in the reducer and equivalent the bearing to a flexible ring with a certain stiffness. The research results showed that the bearing stiffness is the main factor affecting the torsional stiffness of the whole machine. Yang [10] established the finite element model of RV reducer including the stiffness of bearing, the meshing stiffness of gears and the elasticity of each component, and analyzed the influence of the nonlinear characteristics of each component on the torsional stiffness in RV reducer. The literature above mentioned that the torsional stiffness changes periodically with time, but all research did not involve the test of periodic torsional stiffness on RV reducer, and establishment of a complete theory of time-varying torsional stiffness.

The literature above mentioned that the torsional stiffness changes periodically with time, but all research did not involve the test of periodic torsional stiffness on RV reducer, and establishment of a complete theory of time-varying torsional stiffness.

To improve the performance of RV reducer transmission, the investigation of the periodic time-varying stiffness of RV reducer and its application will be carried out in this study, and the contents of this manuscript are arranged as follows: (1) the stiffness fluctuation of RV reducer based on experimental data; (2) the modeling of parametric vibration with single-parameter and double-parameter; (3) observation of the dynamic characteristics of RV reducer through torsional vibration test; (4) application of torsional stiffness fluctuation mechanism of RV reducer.

Variable Torsional Stiffness

Torsional Stiffness Test

Torsional stiffness is expressed by the ratio of the load torque and the corresponding torsion angle of a RV reducer:

$$K = \frac{\mathrm{d}T}{\mathrm{d}\phi}, \tag{1}$$

where K-torsional stiffness (unit: N·m/arcmin), T-torque (unit: N·m), ϕ-torsion angle (unit: arcmin).

Figure 1 shows the torsional stiffness test platform for a RV reducer. The pin shell of the RV reducer 2 is solidly connected to the frame base, and the circumferential motion of the input shaft is restrained by a set screw. The output end is fixedly connected with the torque arm flange 1, and the torque arm flange is fixedly connected with the blocking plate 4. The micrometer gauge 3 is placed in vertical contact with the blocking plate. The pneumatic cylinder 7 is used to apply a tension force perpendicular to the torque arm 5 to generate torque. The tension force is read by the spring tension meter 6.

Three different torque loads (100 N·m, 200 N·m, 300 N·m) are applied to the output end. The torsional angles of the output end corresponding to loads are measured, respectively. Thus, the torsional stiffness is obtained using Eq. (1). Through loosening the set screw, and repeat the above step to obtain a curve of torsional stiffness as shown in Fig. 2.

RV reducer A, B and C are measured, and Fig. 2a, b and c are corresponding records of torsional stiffness. The ratio of the fluctuation value to average torsional stiffness is evaluated as the torsional stiffness fluctuation index. The above curves are corresponding to 9.17%, 11.59% and 4.16%, respectively.

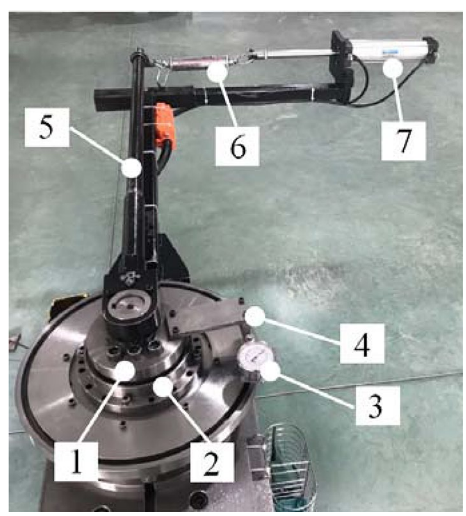

Fig. 1 Static torsional stiffness test device of RV reducers. 1: Torque arm flange, 2: RV reducer, 3: microm gauge, 4: blocking plate, 5: torque arm, 6: spring tension meter, 7: pneumatic cylinder

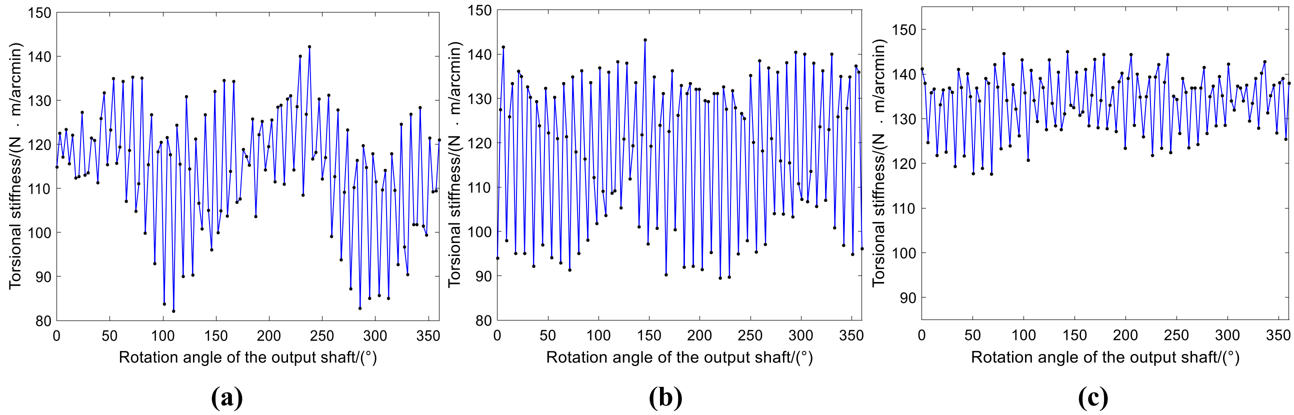

Fig. 2 Torsional stiffness curves measured from three samples of RV reducer

Variable Torsional Stiffness Description

The experimental data of the torsional stiffness in Fig. 2a can be approximately equivalent to the linear superposition of two harmonic functions. As shown in Fig. 3, the low-frequency part is 1.99 periodic wave, namely long-period fluctuation, and the high-frequency part is 40.58 periodic wave, namely short-period fluctuation. The long-period fluctuations also exist in Fig. 2b and c, but this phenomenon is not obvious, while the short-period torsional stiffness fluctuations are all obvious.

Mechanism of Variable Torsional Stiffness

RV Reducer Transmission Structure

Take the RV-40E as the example, it is a two-stage closed planetary gear train composed of the first stage planetary transmission and the second stage cycloid transmission. The high-speed class is a K-H differential gear train consisting of the sun gear 1, two symmetrical planet gears 2 and the tie bar; The low-speed class is a K-H-V planetary gear train consisting of two crankshafts 3, two cycloid gears 4, pin teeth 5 and output shaft 6. The tie bar and the output shaft are fixed as the same part (Fig. 4).

The parameters of the RV reducer: the number of sun gear teeth Z_1 is 12; the number of planet gear teeth Z_2 36; the number of cycloid gear teeth Z_4 39; and the number of pin teeth Z_5 40.

First-order transmission ratio:

$$i_{12} = \frac{n_1}{n_2} = -\frac{Z_1 + Z_5 Z_2}{Z_1 Z_4} \tag{2}$$

Second order transmission ratio:

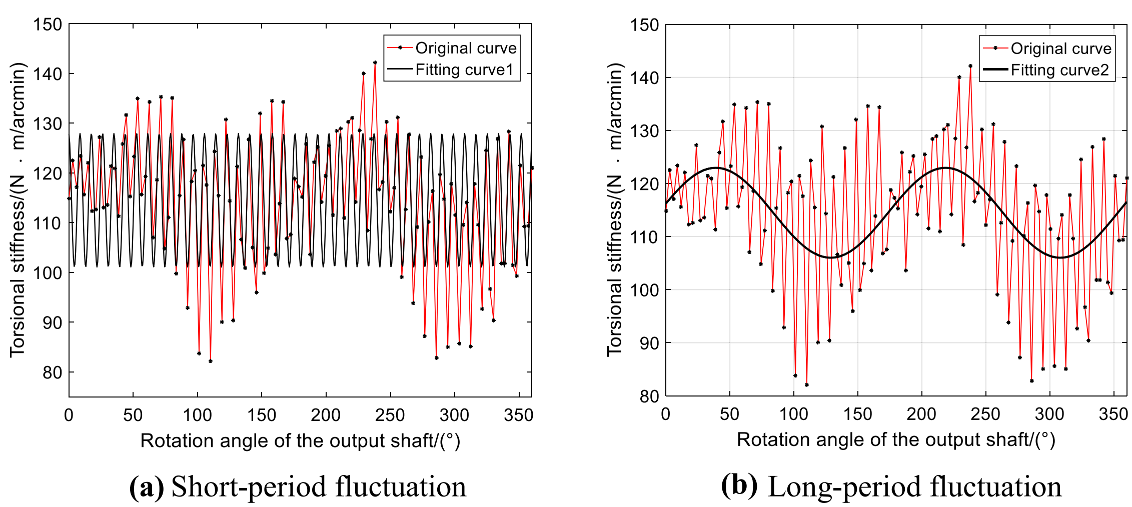

Fig. 3 Torsional stiffness fitting curve of RV reducer

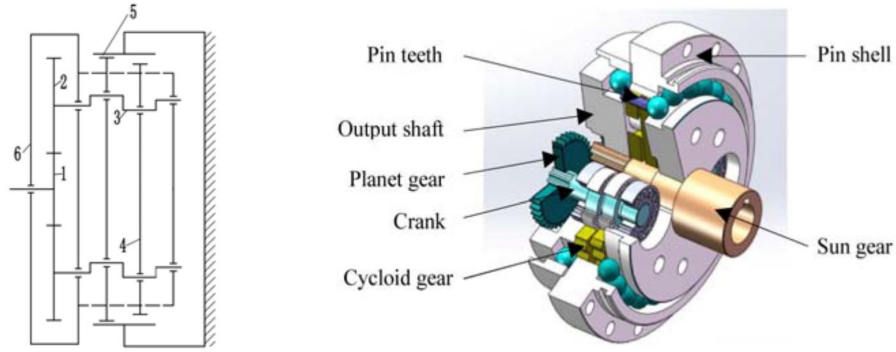

(a) Structure sketch of RV reducer **(b)** 3D model of RV reducer structure

Fig. 4 RV reducer structure

$$i_{45}^{3} = \frac{n_4 - n_3}{n_5 - n_3} = 1 - \frac{n_4}{n_3} = \frac{Z_5}{Z_4} \tag{3}$$

The total transmission ratio of RV reducer:

$$i = \frac{n_1}{n_6} = 1 + \frac{Z_2 Z_5}{Z_1} \tag{4}$$

According to the structure of the RV reducer, the conditions of $n_2 = n_3$ and $n_4 = n_6$ are obtained. The transmission ratio could be calculated as: $i_{12} = \frac{121}{39}$, $i_{34} = 39$.

Short-Period Fluctuation

In the practice, the larger the magnitude of torsional stiffness fluctuation is, the worse the dynamic performance of RV reducer will be. For example, the torsional stiffness fluctuation reduces transmission accuracy, and induces torsional vibration and so on. Therefore, it is necessary to consider what causes the torsional stiffness fluctuation to increase, so as to reduce the torsional stiffness fluctuation by optimizing the design and manufacturing process.

(a) Cycloid transmission uniformity

The fluctuation of the torsional stiffness is in the same period as the fluctuation of the meshing stiffness in the gear system. Therefore, the theoretical frequency of short-period torsional stiffness fluctuation is the cycloid transmission ratio 39, which is close to fluctuation frequency 40.58 in the fitted curve in Fig. 3a.

The working tooth profile of cycloid gears meshes with the pin teeth to produce the torque to bear the load. The uniformity of cycloid transmission is mainly related to the tooth profile deviation of cycloid gears and the diameter error of pin teeth. ZEISS CMM is used to measure and calculate the dimensional error of parts in RV reducer A and C.

The accuracy of the left and right tooth profiles of the cycloid gears is measured, the tooth profile deviation is obtained, as shown in Fig. 5.

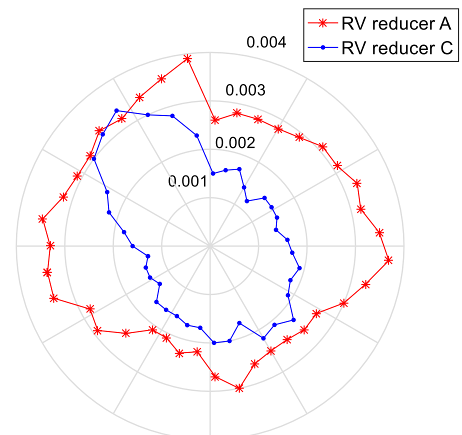

(a) Left tooth profile deviation

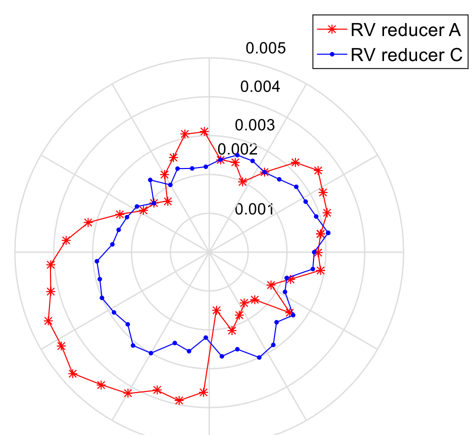

(b) Right tooth profile deviation

Fig. 5 Tooth profile deviation distribution of cycloid gears

The deviation fluctuation can be obtained by calculating the difference between all tooth profile deviation and the one that is closest to the design datum, which can reflect the uniformity of the tooth profile error of the cycloid gears.

Through measurement and statistics, it is concluded that the mean value of deviation fluctuation is 0.872 μm at the cycloid gear's left tooth profile in the RV reducer A, and the mean value of deviation fluctuation is 1.433 μm at the right tooth profile; The mean value of deviation fluctuation is 0.692 μm at the cycloid gear's left tooth profile in the RV reducer C, and the mean value of deviation fluctuation is 0.682 μm at the right tooth profile. The uniformity of tooth profile of the cycloid gear in RV reducer C is obviously better than that in RV reducer A. Better tooth profile uniformity can improve the smoothness of cycloid gear meshing process and reduce torsional stiffness fluctuation.

At the same time, the mean value of the diameter fluctuation is 2.1 μm at the pin teeth in RV reducer A, and that in RV reducer C is 0.25 μm. The diameter fluctuation of pin teeth in RV reducer A is about 8 ~ 10 times of that in reducer C, which will seriously affect the meshing smoothness of cycloid transmission.

(b) The gap between cycloid gears and pin teeth

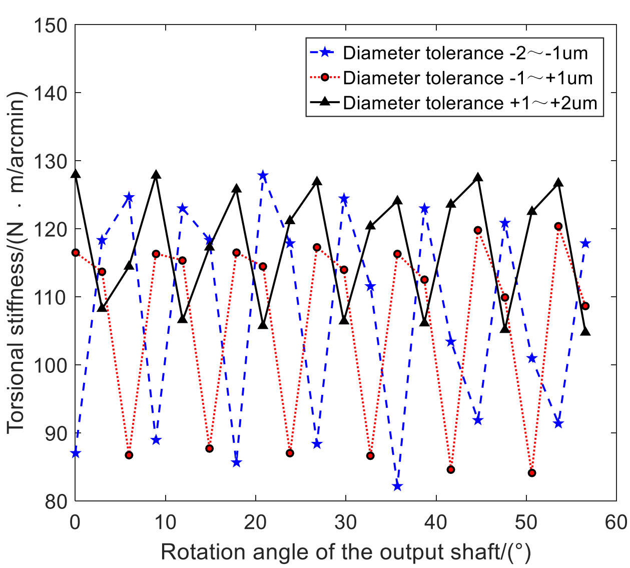

Fig. 6 Torsional stiffness fluctuation related with different pin teeth diameters

In the study, by changing the diameter of the pin teeth to change the fit gap between cycloid gears and pin teeth, the fluctuation magnitude of torsional stiffness can be improved. The torsional stiffness curve under different diameter tolerances of the pin teeth are shown in Fig. 6. Thus, it can be concluded that the gap between cycloid gears and pin teeth decreases, and the fluctuation of torsional stiffness decreases.

However, the diameter of the pin teeth should not be increased too much, otherwise the clearance between the cycloid gears and the pin teeth is too small, it results increment of meshing wear and reduction of transmission efficiency, and even lead to the whole machine jammed. Therefore, to improve the torsional stiffness performance of RV reducer using this method, it is necessary to ensure that the transmission efficiency is not affected.

Long-Period Fluctuation

As shown in Fig. 3b, The period of torsional stiffness fluctuation is approximately 2. The direct reason of long-period fluctuation is the eccentricity of the cycloid gears, which causes the loose-tight meshing with the pin teeth. There are many reasons leading to the eccentricity of the cycloid gears, which can be summarized as follows:

The eccentricity of the sun gear produces extrusion pressure F on the planet gear, as shown in Fig. 7, which causes the center of the double crankshafts to deviate from the original rotating center. The eccentricity of the double crankshafts is shown in Fig. 8. The double crankshafts drive the cycloid gears directly, and its eccentricity causes the cycloid gears the loose-tight meshing with the pin teeth. As shown in Fig. 9a, the initial state is that a cycloid gear is closely engaged with the pin teeth, and the dotted line is used to represent the over-tight meshing. When the cycloid gear rotates for half a cycle, Fig. 9b shows that another cycloid gear is tightly engaged with the pin teeth. Thus, the torsional stiffness fluctuates with a period of 2.

Fig. 7 Eccentricity of the sungear

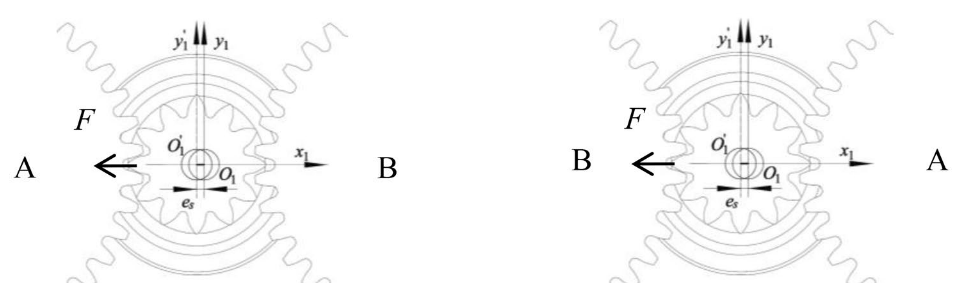

(a) Initial state **(b)** Planet gears running half a circle

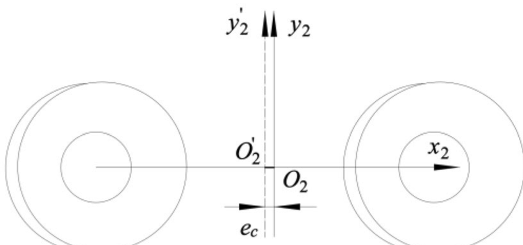

Fig. 8 Eccentricity of the double crankshafts

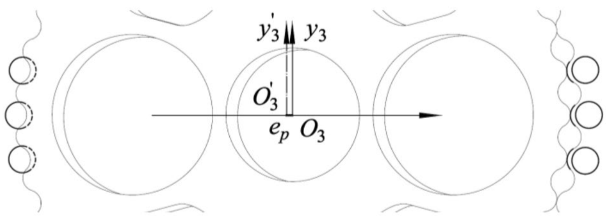

(a) Initial state

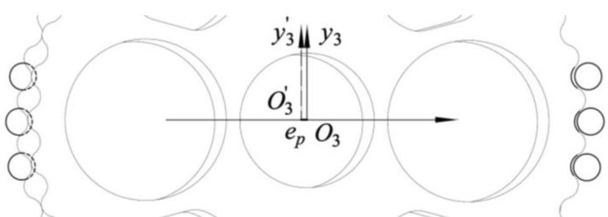

(a) Cycloid gears running half a circle

Fig. 9 Eccentricity of the double cycloid gears

Parametric Vibration Caused by Time-Varying Torsional Stiffness

Parametric Vibration

When the RV reducer works, the torsional stiffness with position periodicity is converted to periodic time-varying torsional stiffness, forming the system parametric torsional vibration. Parametric vibration is a forced vibration response generated by external excitation due to the periodic change of parameters in the system [11, 12].

Taking the test result of torsional stiffness of RV reducer A as an example, the time-varying torsional stiffness function is mathematically described as:

$$K(t) = K_0\left(1 + \beta_1 \cos \omega_{o1} t + \beta_2 \cos \omega_{o2} t\right) \quad (5)$$

where K_0 is the average torsional stiffness, ω_{o1} the frequency of short-period fluctuation, ω_{o2} the frequency of long-period fluctuation, β_1 the short-period torsional stiffness fluctuation index and β_2 the long-period the torsional stiffness fluctuation index.

External excitation torque includes drive torque excitation and load torque excitation [13], which can be described as:

$$M(t) = A \cos \omega_{p1} t + B \cos \omega_{p2} t \quad (6)$$

Thus, the parametric torsional vibration equation is:

$$J \cdot \ddot{\theta}(t) + C \cdot \dot{\theta}(t) + K(t) \cdot \theta(t) = M(t) \quad (7)$$

where J is the moment of inertia of the system, C is the damping, $\theta(t)$ is the angular displacement, and $M(t)$ is the torque.

Parametric Vibration Response and Spectrum Analysis

The torsional parametric vibration equation under the harmonic excitation:

$$\begin{aligned} &\frac{\mathrm{d}^2\theta}{\mathrm{d}t^2} + 2\zeta\omega_n \frac{\mathrm{d}\theta}{\mathrm{d}t} + \omega_n^2\theta(1 + \beta_1 \cos \omega_{o1} t \\ &+ \beta_2 \cos \omega_{o2} t) = A \cos \omega_{p1} t + B \cos \omega_{p2} t \end{aligned} \quad (8)$$

where ζ is the damping ratio, ω_n is the torsional natural frequency. Using frequency response measurement, the first natural frequency of system, with a symmetric moment of inertia of 56.65 kg·m^2, is estimated as19π, and the damping ratio is 0.025. When the driving speed is 1400 rpm, the driving frequency is $\omega_{p1} = 46.66\pi$, and the load torque excitation frequency is $\omega_{p2} = 0.386\pi$; The amplitude of driving excitation A is 1000, and the amplitude of load excitation B is 1000; Meanwhile, the indexes and coefficients in the parametric equations are determined as, $\omega_{o1} = 15.04\pi$, $\omega_{o2} = 0.772\pi$, $\beta_1 = 0.1172$ and $\beta_2 = 0.0764$.

The response of the parametric torsional vibration is solved by Runge–Kutta method, and Fig. 10 shows the time history of steady-state response.

The time-history of the simulation response is obtained at the speed of 1400 rpm, and the corresponding spectrum is obtained, as shown in Fig. 11. Its characteristics are as follows: there is a complex band around the primary frequency [14], which is caused by the torsional stiffness fluctuation. Therefore, the interval between the primary frequency and the band frequency is basically the same, and corresponds to the harmonic combination of $\omega_{o1} = 15.04\pi$ (7.02 Hz) and $\omega_{o2} = 0.772\pi$ (0.386 Hz).

Stability Analysis

The response of the parametric system is sometimes weak, but sometimes stronger resonance phenomenon may occur, which depends on the stability of the parametric system [15].

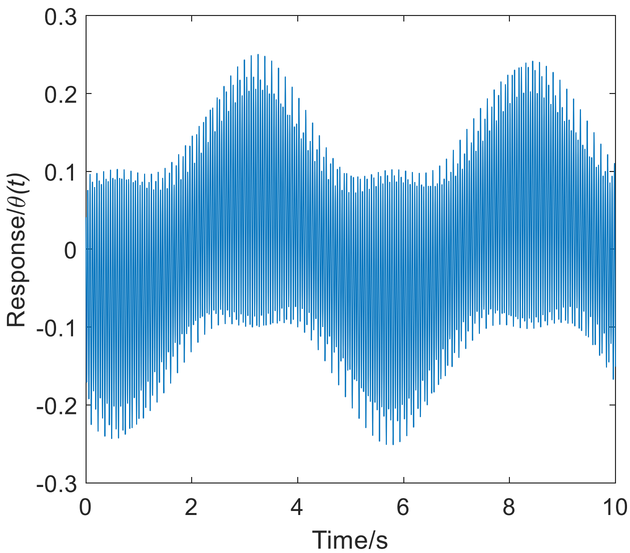

Fig. 10 Time-history of vibration response

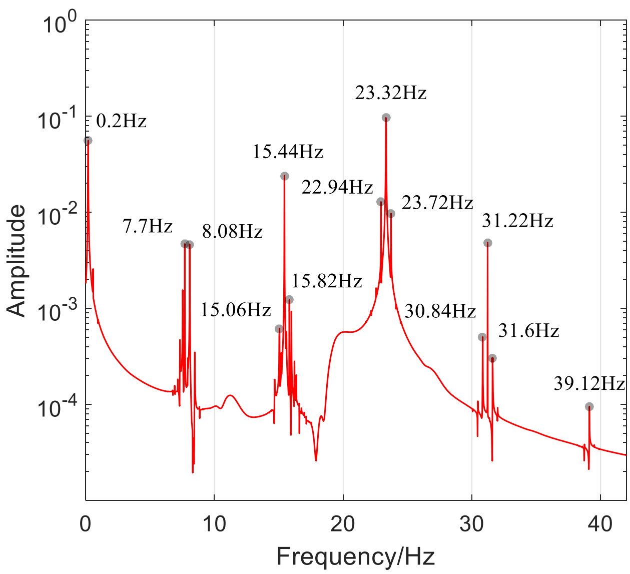

Fig. 11 Spectrum of vibration response

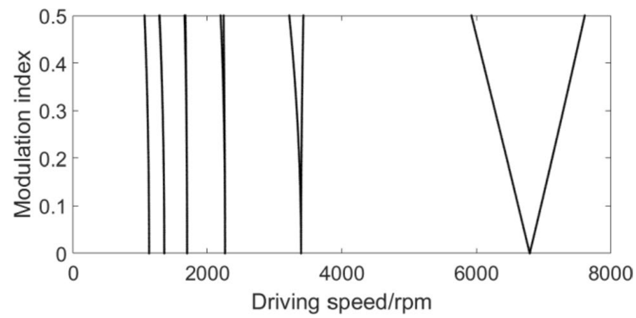

Fig. 12 Instability area under single-parameter excitation ω_{o1}

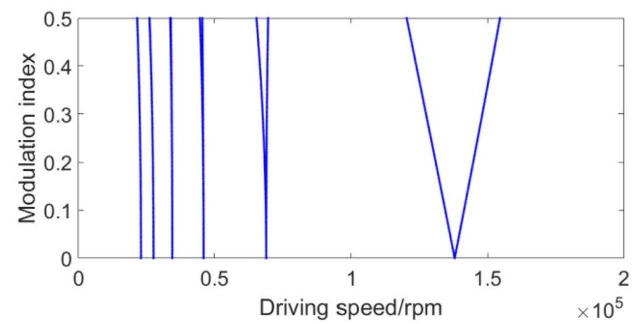

Fig. 13 Instability area under single-parameter excitation ω_{o2}

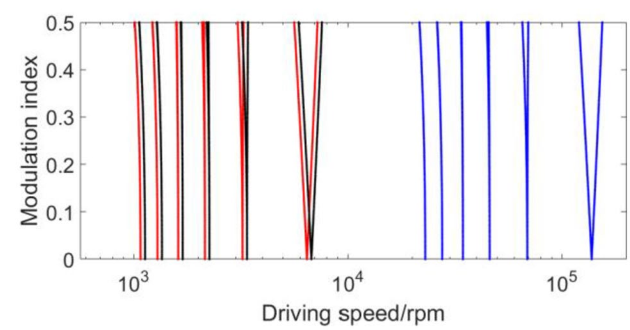

Fig. 14 Instability area under double-parameter excitation

The critical frequency of instability is solved by Fourier series method, and the instability area of torsional vibration is obtained.

The instability diagrams of the parametric system with the excitation parameters ω_{o1} or ω_{o2} is given, as shown in Fig. 12 and Fig. 13. where the x-coordinate represents the driving speed of the motor. It can well reflect the instability area of torsional vibration of the RV reducer system.

The parametric vibration with double-parameter excitation would superimpose the instability area of single-parameter excitation and generate the coupling instability area, as shown in Fig. 14. Because of the action of nonlinear coupling, the instability area of the parametric vibration with double-parameter excitation is greater than the sum of the single-parameter excitation.

Numerical simulation of single-parameter and double-parameter torsional vibration responses are obtained by frequency sweeping. The vibration response and its envelope are shown in Figs. 15 and 16. It should be noted that the amplitude of vibration response with double-parameter excitation is nearly four times that with single-parameter excitation, and the magnitude of vibration response caused

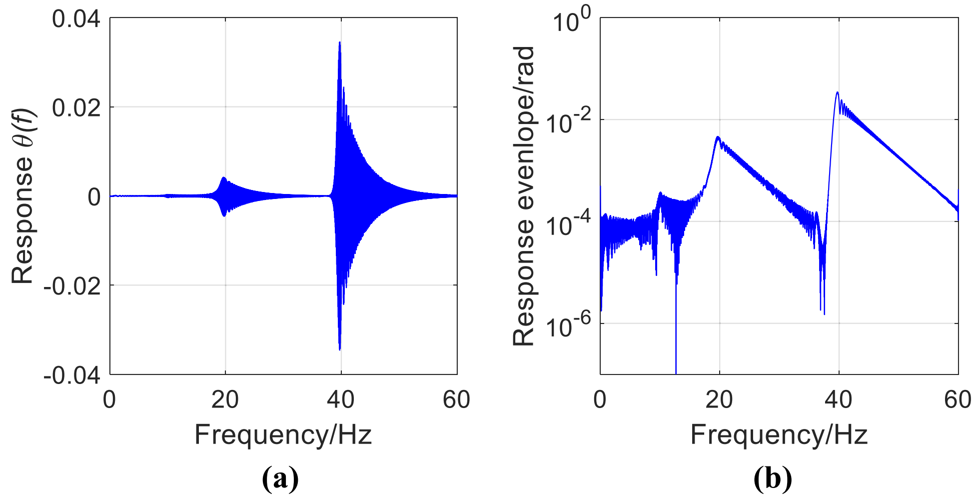

Fig. 15 Vibration response under single-parameter excitation and its envelope

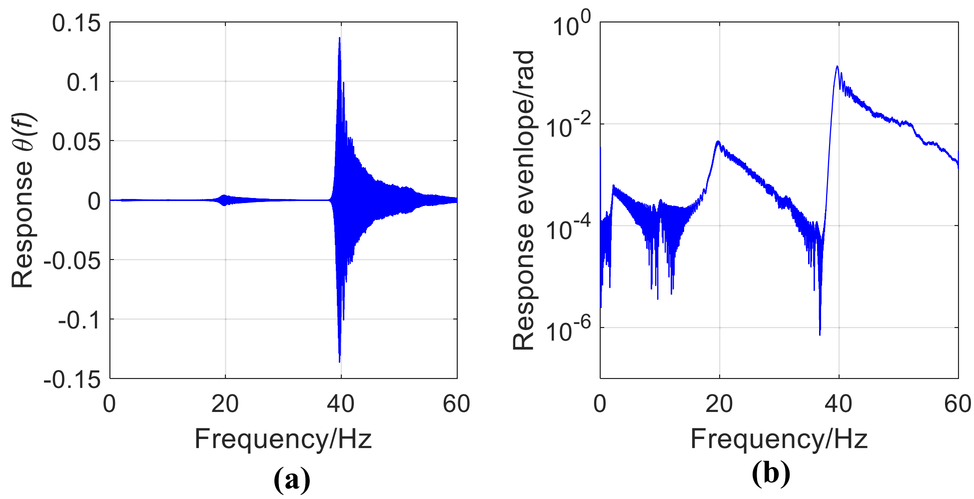

Fig. 16 Vibration response under double-parameter excitation and its envelope

by double-parameter excitation is much larger than single-parameter excitation.

Experiment

To investigate the time-varying stiffness affecting torsional vibration characteristics under actual working conditions, a torsional vibration test device is built for RV reducer. The device is composed of a servo motor, a RV-40E reducer, a test frame, an inertial load, a wireless acceleration sensor and an electric control box, etc., as shown in Fig. 17. When the servo motor is driving, the inertial load arm rotates with the output end of RV reducer. The wireless acceleration sensor is installed on the inertial load arm 550 mm away from the rotating center to pick up the circumferential vibration, which can be considered as the torsional vibration [16].

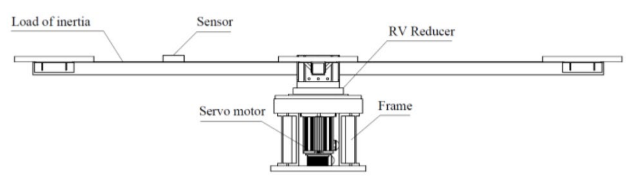

(a) Schematic diagram of test device

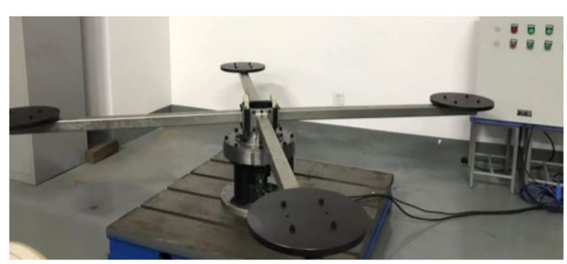

(b) Picture of test device

Fig. 17 Sketch of RV torsional vibration automatic test device

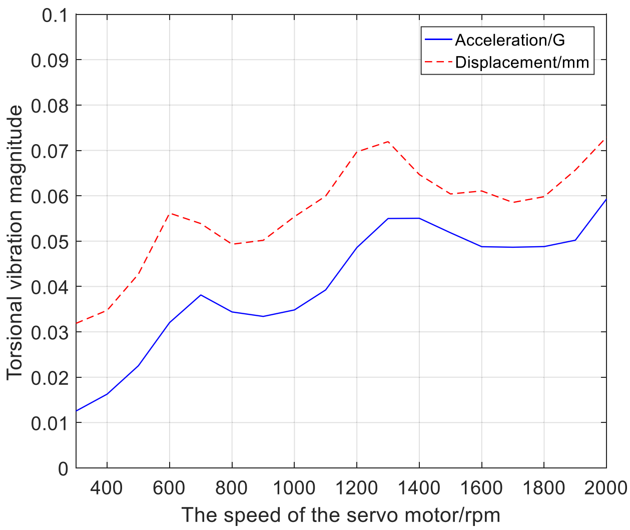

Fig. 18 Torsional vibration–speed characteristic of RV reducer (number A)

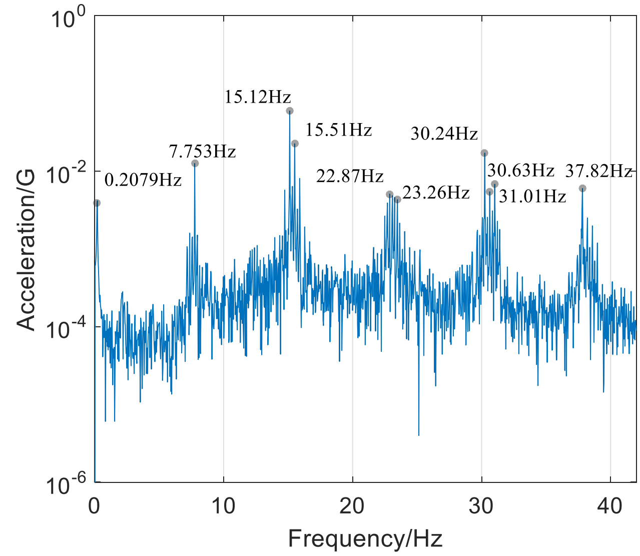

Fig. 20 Band in the spectrum of torsional vibration

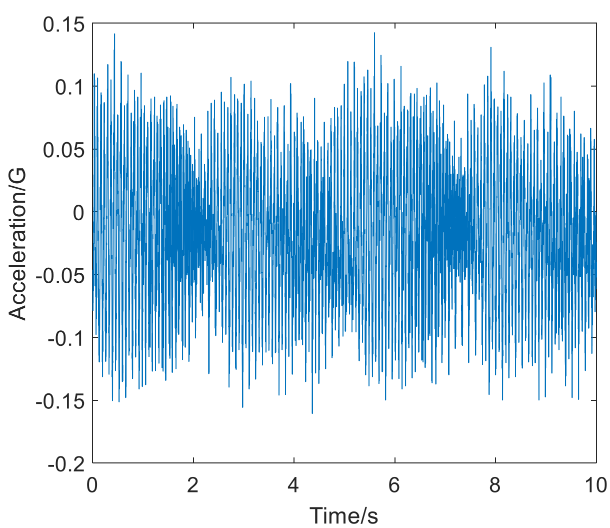

Fig. 19 Time record of torsional vibration

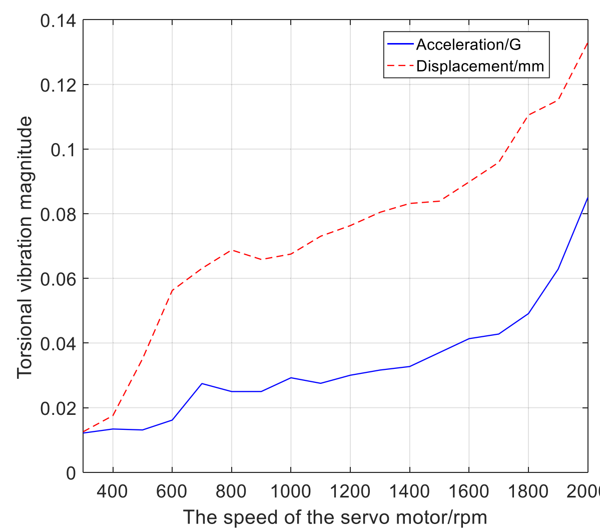

Fig. 21 Torsional vibration-speed curve of the RV reducer

To verify the double-period stiffness fluctuation characteristics of the parametric torsional vibration model, the test is carried out on RV reducer A. The torsional vibration-speed characteristic curves is shown as Fig. 18, it can be found the peak of the curve is very close to the simulation (Fig. 16b).

When the driving speed is 1400 rpm, the time record of torsional vibration (Fig. 19) is collected and the spectrum is analyzed. As shown in Fig. 20, there is an obvious band in the spectrum of torsional vibration, which is due to the combination of internal and external excitation frequencies of the torsional vibration, namely the linear combination of the torsional stiffness fluctuation frequency ($f_{o1} = 7.02$hz, $f_{o2} = 0.386$hz) and the external excitation frequency ($f_{p1} = 23.33$hz, $f_{p2} = 0.193$hz). Compared with the frequency spectrum of simulation (Fig. 11), there is good consistency between their features, and it can be concluded that the band frequencies in the spectrum are all linear combinations of the above excitation frequencies.

Application

The torsional vibration performance curve, i.e. the property of torsional vibration-speed, of an RV reducer is shown in Fig. 21. When the driving speed is 2000 rpm, the torsional

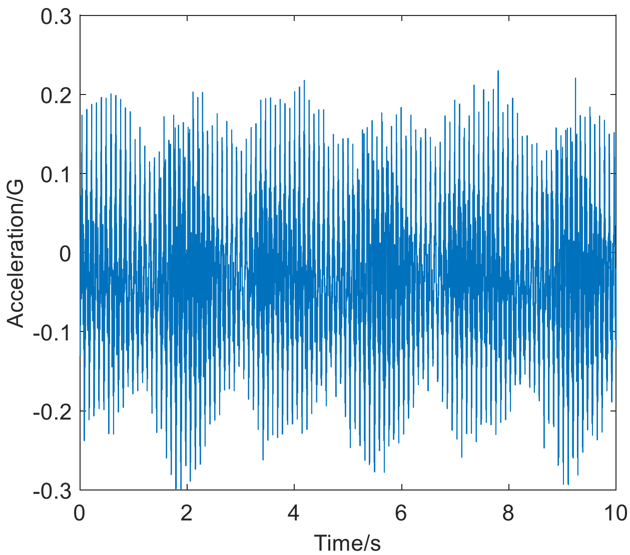

Fig. 22 Time record of torsional vibration

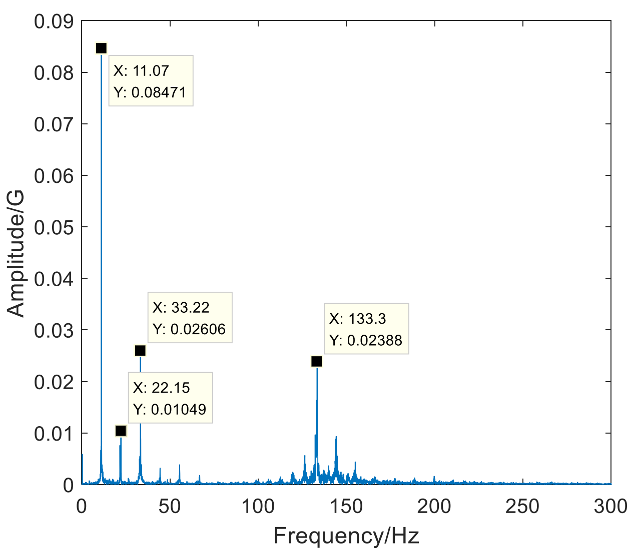

Fig. 23 Frequency spectrum of torsional vibration

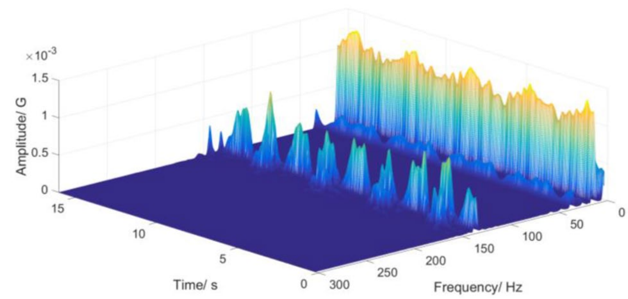

Fig. 24 STFT analysis of torsional vibration

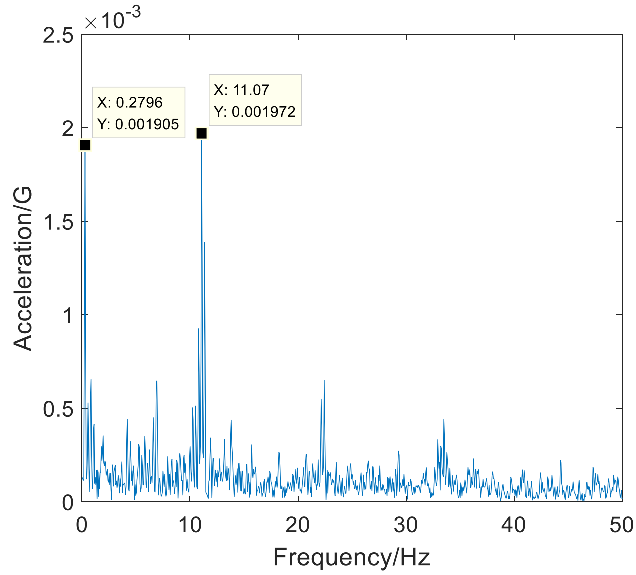

Fig. 25 Envelope spectrum of torsional vibration

vibration displacement reaches the maximum value and exceeds the displacement standard value, which is 0.1 mm.

To analyse the dynamic characteristic of RV reducer, the vibration data is collected at the speed of 2000 rpm, as shown in Fig. 22. Spectrum analysis on vibration is carried out, as shown in Fig. 23. It is found that torsional vibration includes two parts. The low-frequency vibration is based on the frequency bands of 11.07 Hz, and a high-frequency vibration is a group of spectra whose center is 133.3 Hz.

The cycloid meshing error in RV reducer transmission is an exciting source of vibration, which will cause low-frequency vibration corresponding to short-period stiffness fluctuation. It is basically consistent with 11.07 Hz in the spectrum. Because the short-period stiffness fluctuation index is relative high, it leads to the parametric resonance in the torsional vibration of RV reducer at this speed.

The frequency of shock vibration response is relative high, and it is located the high-order modal frequency (the 3rd modal frequency) of RV reducer system. Its wave and spectrum can not be used to diagnose defects directly, so special signal processing is carried out on the torsional vibration.

STFT [17] analysis of the torsional vibration can be used to directly observe the fluctuation in the vibration wave, as shown in Fig. 24. However, no exact characteristic can be evaluated from the figure.

To extract the defect information from the shock response, the envelope analysis is carried out on the vibration response after band filtering. The envelope spectrum is shown in Fig. 25, where the loading torque excitation frequency of 0.279 Hz and short-period stiffness fluctuation

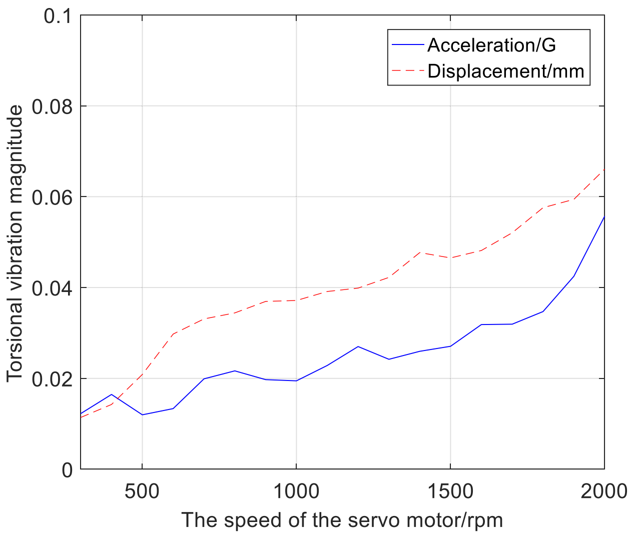

Fig. 26 Torsional vibration–speed curve of the RV reducer (After replacing cycloid gears and crankshafts)

frequency of 11.07 Hz can be obtained. It is concluded that the high-frequency vibration is caused by the joint action of load torque excitation and short-period stiffness fluctuation excitation, so the high-frequency vibration is also related to short-period stiffness fluctuation.

On the above analysis, the dimensions of cycloid gears, crankshafts and pin teeth are measured by a ZEISS Calypso three coordinates measuring instrument. It is found that the tooth profile error in the cycloid gears is beyond 60% of the normal tolerance, the eccentricity of crankshafts exceeds 50% of the normal tolerance. After replacing the crankshafts and cycloid gears in the RV reducer, the torsional vibration test is repeated. Experimental result shows that the reassembly is successful. It can be seen that the displacement value and acceleration value of torsional vibration is significantly reduced to one half of the original one through comparing Fig. 26 with Fig. 21.

Conclusion

The time-varying torsional stiffness of RV reducer is divided into short-period fluctuation and long-period fluctuation. The short-period torsional stiffness fluctuation is caused by cycloid gears meshing. The long-period torsional stiffness fluctuation is caused by the assembly error of the sun gear, crankshafts and cycloid gears.

According to the time-varying stiffness of RV reducer, the parametric torsional vibration equation is established and the dynamic characteristics are analyzed. The correctness of the dynamic model and the mathematical description of time-varying torsional stiffness are verified by the evidences from the experiment data listed as follows: (1) The harmonic combination band of response spectrum in the given dynamic model are highly consistent with that in the RV reducer test. (2) The envelope of instability and harmonic resonance response is matched to the property of torsional vibration-speed in RV reducer (number A). (3) The vibration will be very strong when the time-varying stiffness with double-parameter exciting in RV reducer.

By applying the mechanism of stiffness fluctuation of RV reducer, the defective parts of RV reducer can be quickly diagnosed on line. By replacing defective parts, the torsional vibration of RV reducer is reduced to one half of the original one and its performance is greatly improved. In addition, the correctness of characteristics of torsional stiffness fluctuation is also proved.

There is a correlation between stiffness fluctuation and torsional vibration characteristics in RV reducer transmission. The time-varying torsional stiffness of the reducer will cause the phenomenon of parametric torsional vibration of the reducer, which will cause harmonic resonance and aggravate the torsional vibration of the RV reducer, so the research on time-varying torsional stiffness has practical engineering valuable. In future research, more work will be done on modifying the profile of cycloid gears and solving the optimal clearance to reduce the torsional stiffness fluctuation, which will have great practical significance.

Acknowledgements The authors would like to acknowledge the support of the Chinese National Natural Science Foundation (51575330) and the support and cooperation of Nantong Zhen Kang Welding Electromachinery Co. Ltd.

References

1. Wang T, Tao Y (2014) Research status and industrialization development strategy of chinese industrial robot. Chin J Mech Eng 50(9):1–13
2. Choi H-S, Oh J (2005) A new revolute robot manipulator adapting the closed-chain mechanism. J Robot Syst 22(2):99–109
3. Wang J, Gu J, Yan Y (2016) Study on the relationship between the stiffness of RV reducer and the profile modification method of cycloid-pin wheel. Lecture Notes in Computer Science (including subseries Lecture Notes in Artificial Intelligence and Lecture Notes in Bioinformatics) 9834, 721–735
4. Li L, He W, Wang X et al (1999) Research on high precision RV transmission of robot. China Mech Eng 09:49–50
5. Liu J, Sun T, Qi H (1999) Dynamic model and natural frequency study of RV reducer. China Mech Eng 04:29–31 **(+34)**
6. He W, Lu Y, Wu X (2013) Torsional stiffness calculation of RV reducer based on equivalent model. Mech Transm (in Chinese) 37(09):38–41
7. Zhang D, Wang G, Huang T, Liu J (2001) Kinetic modeling and structural parameter analysis of RV reducer. Chin J Mech Eng 37(01):69–74
8. Park JS (2006) Stiffness and error analysis of the cycloid drive. College of Engineering, Seoul National University, Korea

9. Kim Kyoung-Hong, Lee Chun-Se, Ahn Hyeong-Joon (2010) Torsional rigidity of a cycloid drive considering finite bearing and hertz contact stiffness. Proceedings of the ASME international design engineering technical conferences and computers and information in engineering conference 2009, DETC2009,vol 6, pp 125–130
10. Yang Y, Zhu L, Chen Z et al (2015) Analysis of torsional stiffness characteristics of RV reducer. J Tianjin Univ (Natural Science and Engineering Technology Edition) 48(02):111–118
11. Huang D (2015) Forced response approach of a parametric vibration with a trigonometric series. Mech Syst Signal Process 52–53:495–505
12. Huang D, Liu C, Zhang B (2019) Free response approximation of a 2-DOF parametric vibration system. J Vib Shock 38(13):13–20
13. Wang J, Li R (1998) The theoretical system for the dynamics of the gear system. China Mech Eng 12:61–64 **(+6)**
14. Li Y, Ding K, He G et al (2018) Mechanism of side band modulation in vibration response signal of gear system. Chin J Mech Eng 54(05):105–112
15. Liu Y, Chen L (2001) Nonlinear vibration. Higher Education Press, Beijing, pp 152–178
16. Gu J et al (2019) Manufacturing quality assurance for a rotate vector reducer with vibration technology. J Mech Sci Technol 33(5):1995–2001
17. Malla C, Panigrahi I (2019) Review of condition monitoring of rolling element bearing using vibration analysis and other techniques. J Vib Eng Technol 7:407–414